Patients with common variable immunodeficiency with autoimmune cytopenias exhibit hyperplastic yet inefficient germinal center responses

Neil Romberg, MD,[a,e] Carole Le Coz, PhD,[a] Salomé Glauzy, PhD,[h] Jean-Nicolas Schickel, PhD,[h] Melissa Trofa, BA,[a] Brian E. Nolan, MD,[b] Michele Paessler, DO,[c,f] Mina L. Xu, MD,[i] Michele P. Lambert, MD,[d,e] Saquib A. Lakhani, MD,[j,m] Mustafa K. Khokha, MD,[j,k,m] Soma Jyonouchi, MD,[a,e] Jennifer Heimall, MD,[a,e] Patricia Takach, MD,[g] Paul J. Maglione, MD, PhD,[n] Jason Catanzaro, MD,[j] F. Ida Hsu, MD,[l] Kathleen E. Sullivan, MD, PhD,[a,e] Charlotte Cunningham-Rundles, MD, PhD,[n] and Eric Meffre, PhD[h,l] *Philadelphia, Pa, New Haven, Conn, and New York, NY*

Background: The lack of pathogen-protective, isotype-switched antibodies in patients with common variable immunodeficiency (CVID) suggests germinal center (GC) hypoplasia, yet a subset of patients with CVID is paradoxically affected by autoantibody-mediated autoimmune cytopenias (AICs) and lymphadenopathy.

Objective: We sought to compare the physical characteristics and immunologic output of GC responses in patients with CVID with AIC (CVID+AIC) and without AIC (CVID−AIC).

Methods: We analyzed GC size and shape in excisional lymph node biopsy specimens from 14 patients with CVID+AIC and 4 patients with CVID−AIC. Using paired peripheral blood samples, we determined how AICs specifically affected B-and T-cell compartments and antibody responses in patients with CVID.

Results: We found that patients with CVID+AIC displayed irregularly shaped hyperplastic GCs, whereas GCs were scarce and small in patients with CVID−AIC. GC hyperplasia was also evidenced by an increase in numbers of circulating follicular helper T cells, which correlated with decreased regulatory T-cell frequencies and function. In addition, patients with CVID+AIC had serum endotoxemia associated with a dearth of isotype-switched memory B cells that displayed significantly lower somatic hypermutation frequencies than their counterparts with CVID−AIC. Moreover, IgG$^+$ B cells from patients with CVID+AIC expressed *VH4-34*-encoded antibodies with unmutated Ala-Val-Tyr and Asn-His-Ser motifs, which recognize both erythrocyte I/i self-antigens and commensal bacteria.

Conclusions: Patients with CVID+AIC do not contain mucosal microbiota and exhibit hyperplastic yet inefficient GC responses that favor the production of untolerized IgG$^+$ B-cell clones that recognize both commensal bacteria and hematopoietic I/i self-antigens. (J Allergy Clin Immunol 2018;■■■:■■■-■■■.)

Key words: *Common variable immunodeficiency, autoimmune cytopenias, germinal center responses, somatic hypermutation, B-cell tolerance, commensal bacteria, follicular helper T cell, regulatory T cell*

High-affinity antibodies of specific isotypes are essential protections against a vast diversity of pathogens. Antigen-specific responses often involve generation of germinal centers (GCs) within secondary lymphoid tissues that create a unique environment in which B cells expressing the highest-affinity B-cell receptors capture native antigens from follicular dendritic cells and present them to cognate follicular helper T (T_{FH}) cells.[1,2] Subsequent B-cell proliferation occurs with simultaneous expression of activation-induced cytidine deaminase (AID), which mediates somatic hypermutation (SHM) and class-switch recombination (CSR), leading to affinity-matured isotype-switched antibodies and class-switched memory B cells. Immunocompromised AID-deficient mice and human subjects do not generate mutated, high-affinity antibodies and exhibit hyperplastic GCs and increased frequencies of circulating follicular helper T (cT_{FH}) cells and systemic cytokines that might interfere with tolerance and promote autoantibody production.[3,4] It remains to be determined whether similar GC physiopathology might apply to other primary immunodeficiencies.

Common variable immunodeficiency (CVID) encompasses a heterogeneous group of primary antibody deficiency disorders.[5] Patients with CVID have decreased serum antibody concentrations, poorly protective vaccine titers, and low isotype-switched B-cell frequencies.[5,6] Paradoxically, autoantibodies, including self-reactive IgGs, can be detected in plasma of patients with CVID,[7] and approximately 20% experience autoimmune

From the Divisions of [a]Immunology and Allergy, [b]Rheumatology, [c]Hematopathology, and [d]Hematology, Children's Hospital of Philadelphia; the Departments of [e]Pediatrics, [f]Pathology and Laboratory Medicine, and [g]Medicine, Division of Allergy and Immunology, Perelman School of Medicine at the University of Pennsylvania, Philadelphia; Departments of [h]Immunobiology, [i]Pathology, [j]Pediatrics, [k]Genetics, [l]Medicine, and the [m]Pediatric Genomics Discovery Program, Yale University School of Medicine, New Haven; and [n]the Division of Clinical Immunology, Department of Medicine, Icahn School of Medicine at Mount Sinai, New York.

Supported by grant number K23AI115001 from the National Institutes of Health/National Institute of Allergy and Infectious Diseases (NIH/NIAID), the Jeffrey Modell Foundation (to N.R.), and AI-061093, AI-071087, and AI-082713 from the NIH/NIAID (to E.M.).

Disclosure of potential conflict of interest: The authors declare that they have no relevant conflicts of interest.

Received for publication November 8, 2017; revised May 29, 2018; accepted for publication June 1, 2018.

Corresponding author: Eric Meffre, PhD, Yale University School of Medicine, 300 George St, Rm 353F, New Haven, CT 06511. E-mail: eric.meffre@yale.edu. Or: Neil Romberg, MD, Children's Hospital of Philadelphia, Abramson Research Center, Rm 1216C, Philadelphia, PA 19104. E-mail: rombergn@email.chop.edu.

0091-6749/$36.00

https://doi.org/10.1016/j.jaci.2018.06.012

Abbreviations used
AIC: Autoimmune cytopenia
AID: Activation-induced cytidine deaminase
APC: Allophycocyanin
AVY: Ala-Val-Tyr
CQ: Circularity quotient
CSR: Class-switch recombination
cT_{FH}: Circulating follicular helper T
CVID: Common variable immunodeficiency
GC: Germinal center
HD: Healthy donor
ITP: Immune thrombocytopenia
NHS: Asn-His-Ser
PD-1: Programmed cell death protein 1
PE: Phycoerythrin
PerCP: Peridinin-chlorophyll-protein complex
SHM: Somatic hypermutation
T_{FH}: Follicular helper T
Treg: Regulatory T
Tresp: Responder T

cytopenias (AICs) mediated by autoantibodies targeting either erythrocytes (autoimmune hemolytic anemia), platelets (immune thrombocytopenia [ITP]), or both (Evans syndrome).[5] It is unknown why some patients with CVID generate autoantibodies to hematopoietic self-antigens (CVID+AIC), whereas others do not (CVID−AIC) and whether this could be related to alterations in GC responses.

We report that excisional lymph node biopsy specimens from patients with CVID+AIC display irregularly shaped and hyperplastic GCs, whereas GC structures are scarce, small, and circular in patients with CVID−AIC. Despite large GCs, patients with CVID+AIC harbor fewer isotype-switched B cells with poorly mutated IgG transcripts enriched in autoreactive VH4-34-expressing clones that also recognize commensal bacteria,[8] thereby suggesting that CVID-associated autoimmunity can be triggered by failed containment of mucosal microbiota.

METHODS

Patients

We obtained peripheral blood samples from 44 patients with CVID+AIC and CVID−AIC (see Table E1 in this article's Online Repository at www.jacionline.org). Each patient met 1999 Pan-American Group for Immunodeficiency CVID diagnostic criteria and was receiving antibody replacement therapy but not immunosuppressive medications at the time of enrollment. The average age of enrolled patients with CVID+AIC was 37.1 years (range, 7-68 years), and 48% were male. The average age of enrolled patients with CVID−AIC was 38.5 years (range, 10-67 years), and 35% were male. For purposes of comparison, we also obtained peripheral blood samples from 12 immunocompetent patients with ITP. The group's average age was 19.9 years (range, 8-42 years), and 40% were male. We also obtained plasma samples from 6 AID-deficient patients (average age, 30.4 years [range, 4-60 years; 50% male). Finally, we analyzed peripheral blood samples from 43 related and unrelated healthy donors (HDs) with a mean age of 37.2 years (range, 8-59 years); 41.6% were male.

Patient excisional lymph node biopsy specimens were identified based on review of our CVID cohort's medical records. Fourteen of 18 patients carried a CVID diagnosis at the time of node removal. Lymph nodes from 5 patients (1 patient with CVID+AIC and 4 patients with CVID−AIC) were obtained during breast or thyroid cancer staging before initiation of chemotherapy. All analyzed staging nodes were determined to be malignancy free by a clinical pathologist.

We obtained paired node and blood samples from 14 patients with CVID. In all cases node excision preceded blood sample donation. The mean duration between excision and phlebotomy was 51.9 months (range, 3 months to 14 years). In addition, lymph nodes were obtained from 4 patients who did not donate blood samples. One was an autopsy specimen, another was excised from a patient before hematopoietic stem cell transplantation, and 2 patients did not consent to phlebotomy. Lymph nodes from age-matched control subjects and patients with bacterial lymphadenitis were identified from available clinical pathology cases at Yale New Haven Hospital and the Children's Hospital of Philadelphia. Study protocols were approved by the institutional review boards of Yale University, Mount Sinai, the Children's Hospital of Philadelphia, and the University of Pennsylvania.

Cell staining and sorting, cDNA, RT-PCR, and *VH* sequence analyses

Mononuclear cells were isolated from peripheral blood by using Ficoll density gradient centrifugation, and B cells were enriched with CD20 microbeads (Miltenyi Biotec, Bergisch Gladbach, Germany). B cells were stained with anti-human CD19–Pacific Blue, anti-human CD27–peridinin-chlorophyll-protein complex (PerCP)-Cy5.5, anti-human CD21–allophycocyanin (APC), and anti-human IgG–phycoerythrin (PE; all from BioLegend, San Diego, Calif). Single $CD19^+CD21^+CD27^+IgG^+$ B cells from 12 patients with CVID and 12 HDs were sorted on FACSAria (Becton Dickinson, Franklin Lakes, NJ) or MoFlo Astrios EQ (Beckman Coulter, Fullerton, Calif) flow cytometers into 96-well PCR plates that were immediately frozen on dry ice. RNA from single cells was reverse transcribed in the original 96-well plate in 12.5-μL reactions containing Superscript II RT (Gibco BRL, Grand island, NY) for 45 minutes at 42°C. RT-PCR reactions, including primer sequences, were as described. In brief, IgG gene transcripts were amplified in 96-well plates with 2 rounds of nested PCRs using HotStar Taq DNA polymerase (Qiagen, Hilden, Germany) and 3.5 μL of cDNA as a template for the first PCR reactions and 3.5 μL of PCR1 reaction as a template for the second PCR reactions.[9] *VH* sequences were analyzed by using the National Center for Biotechnology Information IGBLAST software, and *VH4-34* transcripts were aligned to the germline consensus *VH4-34*01* sequence. We especially focused our analysis on the mutational status of the VH4-34 framework region 1 Ala-Val-Tyr (AVY) motif responsible for I/i self-antigen binding and the Asn-His-Ser (NHS) motif in the CDR2 region that modulates antibody affinity to cognate antigens.[8]

Lymph node staining and analysis

Hematoxylin and eosin–stained lymph node sections were analyzed at low power (12.5×) on a DM4000B microscope (Leica Biosystems, Wetzlar, Germany) to capture the node's entire 2-dimensional area with a Spot RT/SE Slider camera (SPOT Imaging, Sterling Heights, Mich). Follicular structures were traced and scored for circularity *in silico* with ImageJ software (National Institutes of Health, Bethesda, Md) by using the following formula:

$$\text{Circularity} = 4\pi\left(\text{Area}/\text{Perimeter}^2\right).$$

Lymph node follicular composition was determined by dividing the combined 2-dimensional areas of all follicular structures by the total lymph node area, excluding adipose-rich or acellular fibrous tissues. All pathologic images were reviewed by 1 or more hematopathologists. Immunohistochemical staining was performed with anti-CD21 (1:100; Dako, Glostrup, Denmark), anti-CD3 (prediluted; Ventana, Oro Valley, Ariz), anti-CD20 (1:200; Dako), and anti-BCL6 (1:50; Dako) antibodies.

In vitro regulatory T-cell suppression assay

$CD4^+$ T cells were enriched with the EasySep Human $CD4^+$ T Cell Enrichment Kit (STEMCELL Technologies, Vancouver, British Columbia, Canada) or the MojoSort Human CD4 T Cell Isolation Kit (BioLegend). $CD4^+CD25^{hi}CD127^{lo/-}$ regulatory T (Treg) cells and $CD3^+CD4^+CD25^-$ responder T (Tresp)

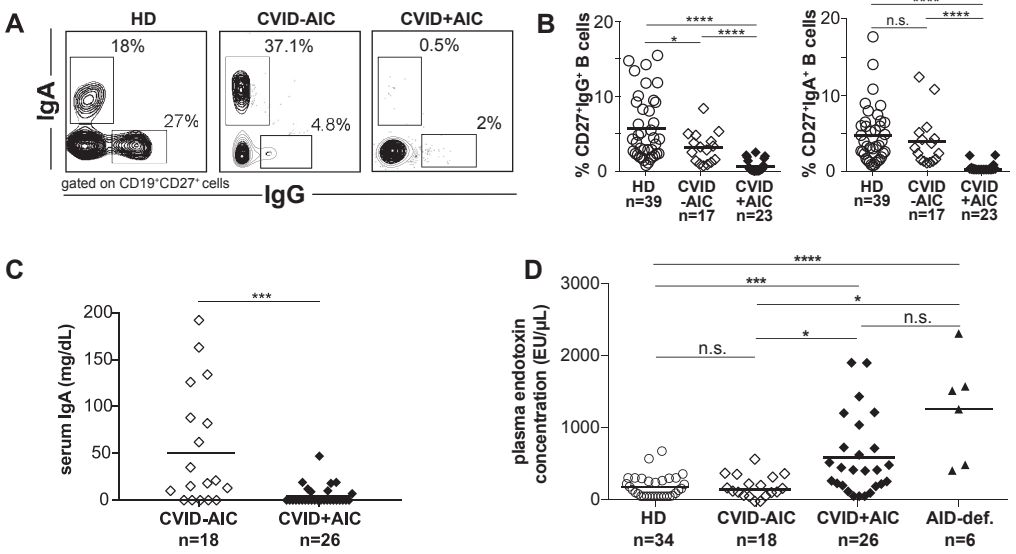

FIG 1. IgA deficiency and increased plasma endotoxin concentrations correlate with AIC development in patients with CVID. **A,** Representative dot plots of IgG and IgA expression on $CD19^+CD27^+$ gated memory B cells from the indicated subjects. **B,** $CD27^+IgG^+$ and $CD27^+IgA^+$ B-cell frequencies in HDs, patients with CVID+AIC, and patients with AIC−AIC displayed as proportions of total circulating B cells. **C** and **D,** Serum IgA (Fig 1, *C*) and plasma endotoxin (Fig 1, *D*) concentrations are shown. *Dark bars* represent average group values. Statistically significant differences are indicated as follows: $*P < .05$, $***P < .001$, and $****P < .0001$, Mann-Whitney U test. *n.s.*, Not significant.

cells were sorted by using flow cytometry and labeled with carboxyfluorescein diacetate succinimidyl ester (Thermo Fischer, Waltham, Mass). Treg and Tresp cells were cocultured at a 1:1 ratio with beads loaded with anti-CD2, anti-CD3, and anti-CD28 (Treg Suppression Inspector Human; Miltenyi Biotec). Cocultures were stained for viability with the LIVE/DEAD kit (Thermo Fisher), and proliferation of viable Tresp cells was analyzed for carboxyfluorescein diacetate succinimidyl ester dilution at 3.5 to 4.5 days.

Flow cytometry

The following antibodies were used for flow cytometric staining: anti-CD19 APC-Cy7, anti-CD27 PerCP-Cy5.5, anti-CD21 Pacific Blue, anti-CD4 APC-Cy7, anti-CD25 PE-Cy7, PE or PE Dazzle, anti-CD127 PerCP-Cy5.5 or APC, anti-CD45RO AF-700, anti-CXCR5 Pacific Blue, anti–programmed cell death protein 1 (PD-1) PE-Cy7 (all from BioLegend), anti-CD3 eFluor 605NC (eBioscience, San Diego, Calif), and anti-IgG APC (Becton Dickinson). Intracellular staining with anti-Foxp3 Alexa Fluor 488 (eBioscience) or APC (BioLegend) was performed by using the Foxp3/Transcription Factor Staining Buffer Set (eBioscience), according to the manufacturer's instructions.

Endotoxin quantification

Endotoxin concentrations were determined in plasma samples by using the Pierce LAL chromogenic endotoxin quantification kit (Thermo Fischer).

Statistics

Data were analyzed with GraphPad Prism software (GraphPad Software, La Jolla, Calif) by using either Mann-Whitney *U* tests or linear regression analysis.

RESULTS

IgA deficiency and endotoxemia correlate with AIC development in patients with CVID

To determine what humoral alterations promote CVID+AIC, we analyzed peripheral B cells from 26 patients with CVID+AIC and compared them with counterparts from 18 age-matched patients with CVID−AIC and 43 HD control subjects. The CVID+AIC group included 8 patients with Evans syndrome, 2 patients with autoimmune hemolytic anemia, and 16 patients with ITP, whereas 8 of 18 patients with CVID−AIC experienced other noncytopenic inflammatory diseases (see Table E1). The majority of enrolled patients with CVID lacked a molecular diagnosis, although some pathologic mutations in CVID-associated genes, including *CTLA4*, *NFKB1*, and *TNFRSF13B*, were identified mostly within the CVID+AIC group (see Table E1). Our CVID+AIC cohort displayed increased frequencies of $CD19^{hi}CD21^{-/lo}$ B cells compared with patients with CVID−AIC (25.0% vs 3.8%, $P < .0001$; see Fig E1 in this article's Online Repository at www.jacionline.org). This B-cell subset, which was reported to be hyporesponsive *in vitro*, is enriched in autoreactive clones and predicts the development of AICs and splenomegaly in group Ia CVID, a patient subset defined by the Freiburg classification criteria.[6,10,11] In addition, we found more severely decreased $CD27^+IgG^+$ memory B-cell frequencies in patients with CVID+AIC (on average, 0.6% of total B cells) compared with patients with CVID−AIC (2.8%) and HDs (5.4%; $P < .01$ and $P < .0001$, respectively; Fig 1, *A* and *B*). IgA^+ B cells were also consistently scarce in patients with CVID+AIC, averaging only 0.3% of total B cells ($P < .0001$ vs control subjects), whereas patients with CVID−AIC had average frequencies similar to those of age-matched control subjects (3.4% vs 4.4%; Fig 1, *A* and *B*).

Patients with CVID+AIC were uniformly IgA deficient, with an average serum concentration of 4.8 mg/dL, whereas the average concentration in patients with CVID−AIC was significantly greater (50.8 mg/dL, $P < .001$; Fig 1, *C*). Because IgA antibodies contain commensal microbiota within the intestinal lumen and at other mucosal sites,[12] we tested whether patients with CVID+AIC with the lowest serum IgA concentrations and

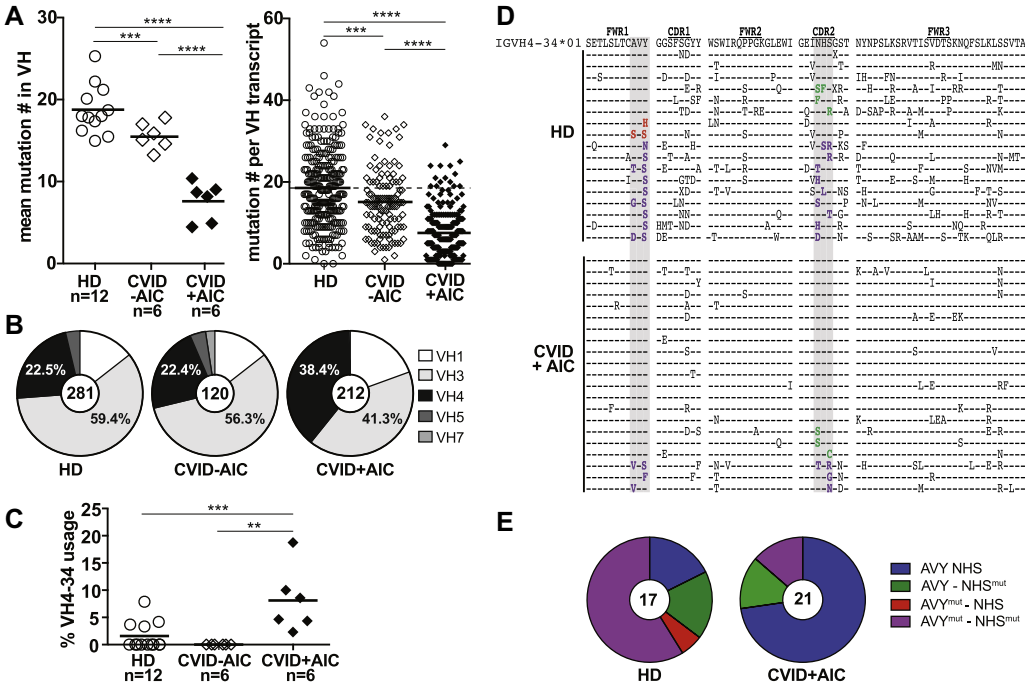

FIG 2. IgG$^+$ B cells from patients with CVID+AIC have low SHM frequencies and an altered *VH* repertoire. **A,** Mutations in *VH* transcripts from CD27$^+$IgG$^+$ B cells from 12 HDs *(open circles)*, 6 patients with CVID−AIC *(open diamonds)*, and 6 patients with CVID+AIC *(black diamonds)* are displayed as averaged mutation number per subject *(left)* and absolute mutation number per transcript *(right)*. *Black bars* represent mean values. **B,** Pie charts represent *VH* family gene segment use from pooled IgG transcripts. Transcript numbers per group are indicated in each pie's center. **C,** Averages of *VH4-34* gene segment use in IgG$^+$ B cells. **D,** VH4-34 amino acid sequence alignment for IgG$^+$ memory B cells from HDs and patients with CVID+AIC relative to germline *IGHV4-34*01 (top)*. Identity to germline is denoted by a *dash*, and substituted residues are indicated in black unless within the critical AVY or NHS motifs *(gray columns)*, where text color is red or green, respectively. Substitutions within both motifs are indicated in purple. **E,** Pie charts represent proportions of pooled transcripts in HDs and patients with CVID+AIC with AVY and/or NHS substitutions. Statistically significant differences are indicated as follows: $^{**}P < .01$, $^{***}P < .001$, and $^{****}P < .0001$, Mann-Whitney *U* tests.

circulating IgA$^+$ memory B-cell frequencies displayed bacterial endotoxins in their blood. Indeed, we found significantly increased endotoxin concentrations in the plasma of patients with CVID+AIC, which averaged 482 EU/μL and showed a concentration range similar to those in AID-deficient patients with undetectable serum IgA. Patients with CVID−AIC had endotoxin levels similar to those in HDs (198 EU/μL vs 133 EU/μL; Fig 1, *D*). We conclude that scarce IgA$^+$ B cells, low serum IgA concentrations, and endotoxemia specifically correlate with AIC development in patients with CVID.

IgG$^+$ B cells from patients with CVID+AIC express nontolerized *VH4-34*-encoded antibodies reported to recognize the hematopoietic I/i self-antigen and commensal bacteria

Because patients with CVID+AIC had severely decreased class-switched memory B cells and resembled patients deficient for AID, which mediates CSR and SHM, we analyzed SHM frequencies in single IgG$^+$ B cells isolated from 6 patients with CVID+AIC, 6 patients with CVID−AIC, and 12 age-matched HDs (see Tables E2-E15 in this article's Online Repository at www.jacionline.org). As previously reported by others, we found that patients with CVID generally displayed lower SHM frequencies in heavy chain variable regions *(VH)* than control subjects (Fig 2, *A*).[13,14] IgG *VH* transcripts from patients with CVID+AIC showed the least SHM both when averaged by subject and in pooled sequences, with an average of only 7.5 mutations per *VH* segment compared to 15.1 mutations for patients with CVID−AIC and 18.6 mutations for HDs (patients with CVID+AIC vs patients with CVID−AIC, $P < .0001$; patients with CVID+AIC vs HDs, $P < .0001$; Fig 2, *A*).

We also analyzed our cohort's IgG$^+$ B-cell *VH* repertoires and found *VH3* gene segments to be most used, followed by *VH4* segments, with a *VH3/VH4* use ratio of 2.5:1 in both the HD and CVID-AIC groups (Fig 2, *B*).[8,15] In contrast, CVID+AIC IgG$^+$ B cells favored *VH4* gene segment use with a *VH3/VH4* ratio of 1:1 (Fig 2, *B*). This difference was driven by increased use of the *VH4-34* gene segment identified in 9.9% of CVID+AIC *IgG* transcripts, whereas *VH4-34* gene segments were rarely found in HD and CVID−AIC counterparts (Fig 2, *C*, and see Fig E2 in this article's Online Repository at www.jacionline.org).[8] *VH4-34*–encoded antibodies are intrinsically autoreactive and bind the conserved I/i carbohydrate self-antigen expressed by erythrocytes and other hematopoietic cells; self-antigen recognition relies on the AVY motif in their framework region 1 independently of IgH complementarity determining region 3 and associated light chains.[16-18] A second VH4-34 motif,

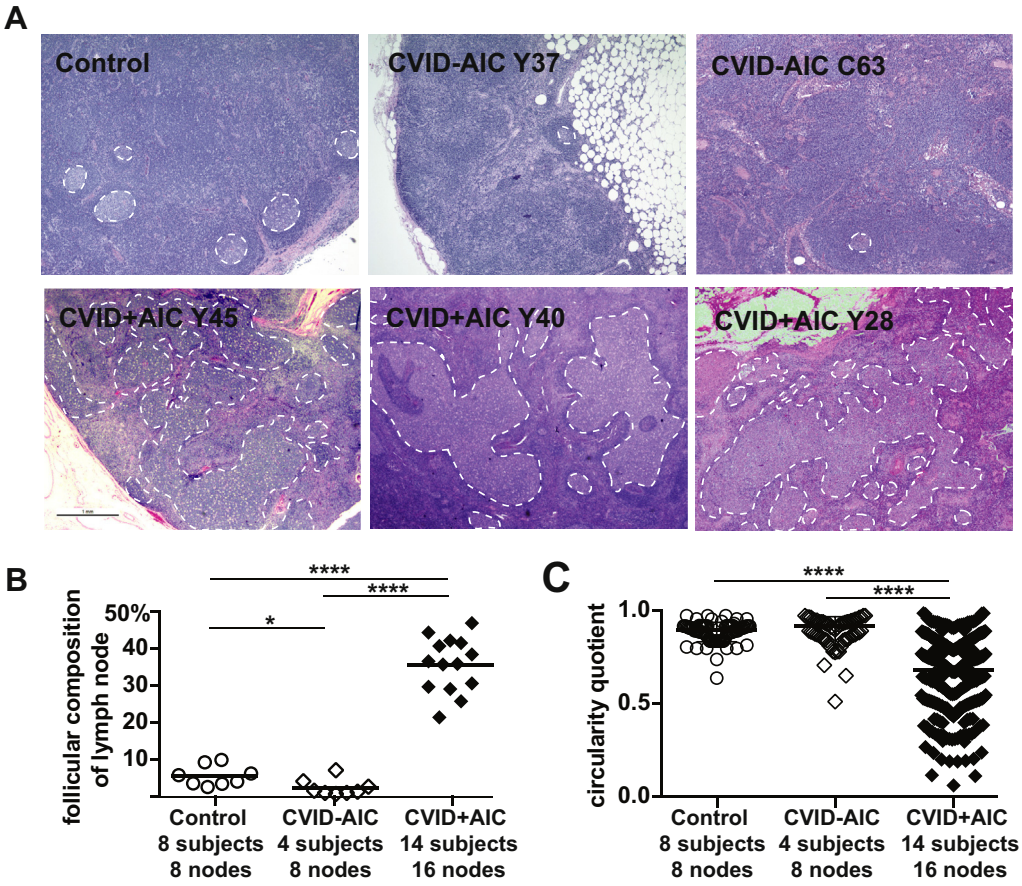

FIG 3. Asymmetric enlarged GCs predominate in lymph nodes from patients with CVID+AIC. **A,** Hematoxylin and eosin–stained axillary lymph node biopsy specimens from a representative immunocompetent 43-year-old woman (control subject), 2 patients with CVID−AIC, and 3 patients with CVID+AIC. GCs are outlined with *white dashed lines*. Original magnification ×12.5. **B** and **C,** Percentages of each lymph node's cellular 2-dimensional surface comprised by GCs (Fig 3, *B*) and each GC's CQ (Fig 3, *C*) are represented for control subjects and patients. Statistically significant differences are indicated as follows: **P* < .05 and *****P* < .0001, Mann-Whitney *U* tests.

Asn-X-Ser (NHS) located in CDR2, modulates antibody/antigen avidity.[18] *VH4-34*–encoded IgG antibodies also often recognize commensal bacteria when AVY and NHS motifs are unmutated.[8]

To determine how SHM differentially modifies these motifs in HDs versus patients with CVID+AIC, we aligned *VH4-34* IgG transcripts with the germline consensus *VH4-34*01* sequence (Fig 2, *D*). Although HD *VH4-34* IgG transcripts displayed nonsynonymous mutations in 64.6% of AVY motifs and 76.4% of NHS motifs, we identified these mutations in only 14.2% of AVY motifs and 28.4% of NHS motifs in VH4-34–expressing B cells from patients with CVID+AIC, who therefore appear to have undergone systemic IgG responses targeting mucosal microbiota (Fig 2, *D* and *E*). Hence AIC development correlates with the presence of VH4-34–expressing IgG^+ B cells with unmutated AVY and NHS motifs that likely recognize both I/i self-antigen and translocated commensal bacteria.

Hyperplastic and irregularly shaped GC responses specifically correlate with patients with CVID+AIC

AID deficiency–associated loss of SHM results in hyperplastic GC responses caused by sustained antigenic B-cell activation in the absence of competitive, mutated, high-affinity antibodies.[3,4] To determine whether severely decreased SHM in patients with CVID+AIC affect their GC responses, we visualized GCs *in situ* through analysis of rare excisional lymph node biopsy specimens from 18 patients with CVID, 14 of whom donated blood samples for memory B-cell analyses. In total, 24 malignancy-free lymph nodes from patients with CVID, which were removed to evaluate lymphadenopathy or for cancer staging before chemotherapy, were analyzed. For comparison, we also obtained malignancy-free control axillary lymph nodes from 4 immunocompetent patients (28-43 years old). Hematoxylin and eosin–stained control lymph nodes displayed distinct and well-spaced GCs comprising approximately 5% (range, 1.6% to 9.5%) of a node's cellular area (Fig 3, *A* and *B*). These structures were scarcer in nodes from patients with CVID−AIC, occupying only 2% of the surface area (range, 0.2% to 1.9%; $P < .01$; Fig 3, *A* and *B*, and see Fig E3 in this article's Online Repository at www.jacionline.org). In contrast, GCs from patients with CVID+AIC were hyperplastic, covering an average of 32.9% (range, 18.5% to 44.4%) of node area ($P < .001$; Fig 3, *A* and *B*, and see Fig E4 in this article's Online Repository at www.jacionline.org).

In addition, *in silico* 2-dimensional scoring of control node GC shape generated an average circularity quotient (CQ) of 0.92 (range, 0.87-0.98), whereas a perfect circle would generate a

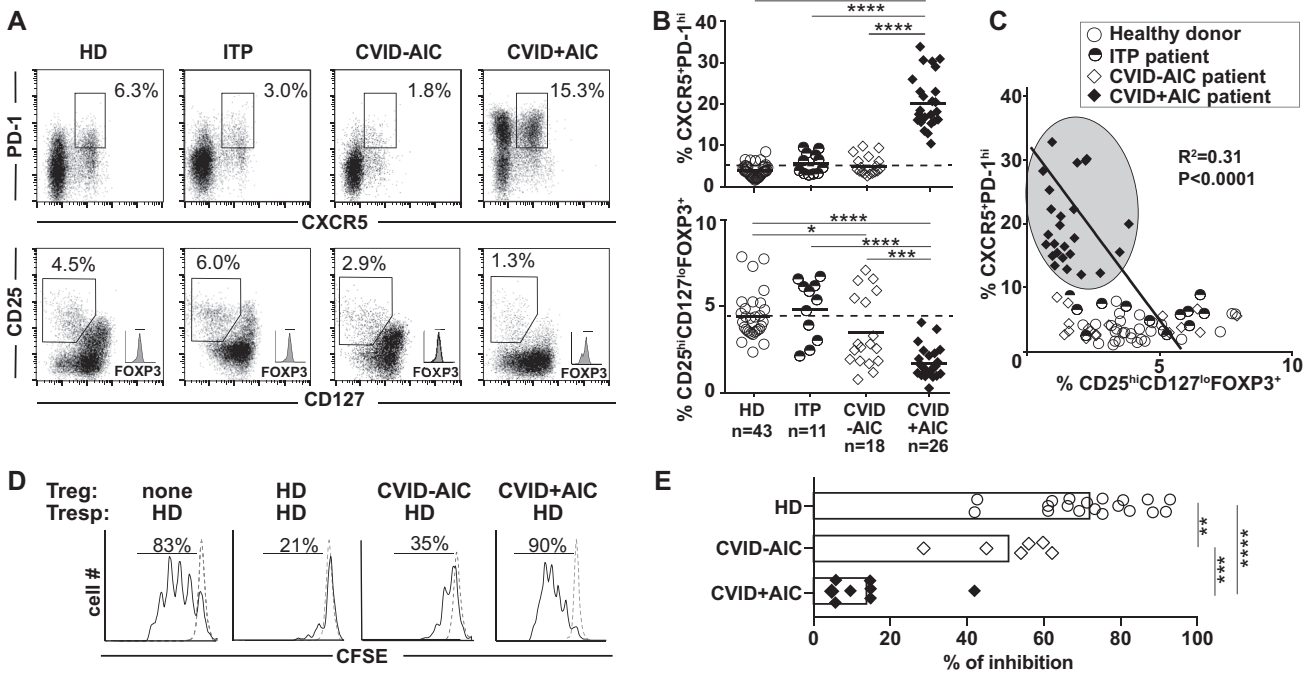

FIG 4. Patients with CVID+AIC have expanded cT_{FH} and decreased Treg cell compartments. **A,** Dot plots show CXCR5/PD-1 *(top)* and CD127/CD25 *(bottom)* expression on gated $CD4^+$ T cells from representative HDs, patients with ITP, patients with CVID−AIC, and patients with CVID+AIC. **B,** Summarized frequencies of $CD4^+CXCR5^+PD\text{-}1^{hi}$ cT_{FH} and $CD4^+CD25^{hi}CD127^{lo}FOXP3^+$ Treg cells in HDs and patients. *Black bars* indicate averages. **C,** Bivariate analysis of paired cT_{FH} and Treg cell frequencies reveal that patients with CVID+AIC segregate in a specific cT_{FH} cell–rich and Treg cell–poor area *(gray oval)*. **D,** Representative histograms of heterologous carboxyfluorescein diacetate succinimidyl ester *(CFSE)*–labeled HD Tresp cell proliferation on day 4 cocultured or not with $CD4^+CD25^{hi}CD127^{lo}$ Treg cells from representative subjects. *Dashed lines* show unstimulated Tresp cells. **E,** Summarized percentages of inhibition by Treg cells from 19 HDs, 7 patients with CVID−AIC, and 7 patients with CVID+AIC are represented. Statistically significant differences are indicated as follows: $*P < .05$, $**P < .01$, $***P < .001$, and $****P < .0001$, Mann-Whitney *U* tests or linear regression analysis.

CQ of 1 (Fig 3, *C*). CVID-AIC nodes also displayed circular-shaped GCs (average CQ, 0.91; range, 0.88-0.96), whereas irregularly shaped GCs were common in CVID+AIC nodes, as shown by their reduced CQ score (0.67; range, 0.09-0.9; $P < .0001$ for both comparisons; Fig 3, *C*). Many GCs from patients with CVID+AIC formed highly complex shapes potentially, suggesting coalescence of multiple GC reactions, yet immunohistochemical staining of these structures for CD20, CD3, BCL6, and CD21 suggested conventional GC cellular organization (see Fig E5 in this article's Online Repository at www.jacionline.org). Despite differences in age, lymph nodes from children with CVID+AIC (n = 1, 7 years old) and adolescents with CVID+AIC (n = 2, 14 and 15 years old) appeared histologically similar to nodes from adults with CVID+AIC and quite dissimilar from age-matched control nodes.

Because GCs enlarge in response to infection, we also obtained 3 reactive lymph nodes from immunocompetent patients with cervical or axillary bacterial lymphadenitis to compare with lymph nodes from patients with CVID+AIC. Indeed, bacterial lymphadenitis resulted in numerous larger GCs comprising a greater average percentage of node cross-sectional area than GCs in control nodes (19.6% vs 5%, $P < .05$; see Fig E6, *A* and *B*, in this article's Online Repository at www.jacionline.org). However, unlike many GCs from patients with CVID+AIC, these structures remained uniformly circular (average CQ score, 0.94; range, 0.86-0.97; see Fig E6, *C*). We conclude that patients with CVID+AIC have hyperplastic GCs with irregular shapes inconsistent with typical lymphadenitis, whereas patients with CVID−AIC demonstrate weak follicular responses.

Expanded cT_{FH} cells combined with a dearth of Treg cells predict follicular hyperplasia and AICs in patients with CVID

Hyperplastic GC reactions in AID-deficient patients correlate with increased numbers of $CD4^+CXCR5^+PD\text{-}1^{hi}$ cT_{FH} cells, which normally promote B-cell survival, proliferation, and SHM.[3] Previously, we reported that patients with CVID with heterozygous *TNFRSF13B* mutations and many with AICs displayed increased cT_{FH} frequencies, but we did not assess whether this feature was associated with AICs or dysregulated GC reactions.[7,19] Therefore we compared cT_{FH} frequencies in patients with CVID+AIC and patients with CVID−AIC, immunocompetent patients with ITP, and HDs. We found cT_{FH} frequencies were significantly increased in patients with CVID+AIC (range, 10.2% to 32.9%) compared with those in patients with CVID−AIC, patients with ITP without CVID, and HDs (1.3% to 9.6%, $P < .0001$; Fig 4, *A* and *B*). In addition, although Treg cells represented around 5% of $CD4^+$ T compartments from HDs and patients with

ITP, Treg cell frequencies were significantly decreased in patients with CVID, especially with AICs (Fig 4, *B*). Bivariate analysis of cT_{FH} and Treg cell frequencies from HDs, immunocompetent patients with ITP, and patients with CVID revealed an inverse and linear relationship between these variables ($R^2 = 0.31$, $P < .0001$), with values assigned to patients with CVID+AIC forming a unique cluster defined by cT_{FH} cell abundance and Treg cell paucity (Fig 4, *C*). Moreover, $CD4^+CD25^{hi}CD127^{lo}$ Treg cells from patients with CVID+AIC did not suppress the *in vitro* proliferation of HD Tresp cells, whereas Treg cells from patients with CVID−AIC showed intermediate suppressive capacities (Fig 4, *D* and *E*). Thus AIC development in patients with CVID correlates with an expanded cT_{FH} cell compartment combined with quantitative and qualitative Treg cell alterations.

Key messages

- **Patients with CVID+AIC have enlarged and irregularly shaped GCs, whereas patients with CVID−AIC demonstrate hypoplastic GCs.**
- **Despite follicular hyperplasia, patients with CVID+AIC generate few isotype-switched B cells with a low frequency of SHMs.**
- **An IgA deficiency–associated failure to contain mucosal microbiota might generate systemic immune responses in patients with CVID+AIC favoring the production of nontolerized VH4-34–expressing IgG^+ B cells recognizing both commensals and hematopoietic I/i self-antigens.**

DISCUSSION

We show here that AIC development in patients with CVID is associated with hyperplastic and irregularly shaped GCs, which correlate with reduced IgA levels, endotoxemia, increased cT_{FH} cell frequencies, dearth of Treg cell, and severely reduced isotype-switched memory B-cell compartments containing decreased SHM and enriched in nontolerized autoreactive VH4-34–expressing IgG^+ clones. Several of these features were identified previously in AID-deficient patients and in patients with CVID with lymphadenopathy/tonsillar hyperplasia and are likely linked to altered SHM.[3,7,20,21] Abrogated and decreased SHM caused by either inborn AID deficiency or poor AID induction previously described in B cells from patients with CVID,[22] respectively, diminishes generation of high-affinity antibodies that normally constrain GC reactions by either competing with GC B cells for binding sites on specific follicular dendritic cell−provided antigens and/or by forming inhibitory immune complexes that co-crosslink B-cell receptors and inhibitory FcγRIIb receptors.[2,3,23] Hence prolonged B-cell activation when SHM is either impaired or decreased likely favors T_{FH} cell expansion and secretion of IL-4, IL-21, and inflammatory cytokines that can alter Treg cell function.[3,7]

Decreased SHM combined with defective CSR also limits anticommensal IgA production that might result in failed mucosal microbiota containment, especially in the gut, further inducing systemic immune responses involving GCs.[8] In agreement with this hypothesis, high plasma levels of endotoxins were reported previously in patients with CVID before IgG replacement therapy.[24] Among our IgG-replete cohort, we found increased bacterial endotoxin plasma concentrations specifically in IgA-deficient patients with CVID+AIC who also possessed $VH4\text{-}34^+IgG^+$ B cells with unmutated AVY and NHS motifs, which have been reported recently to recognize commensal bacteria.[8] Because these AVY- and NHS-unmutated $VH4\text{-}34^+$ IgG clones are also autoreactive and recognize the I/i self-antigens expressed on the surfaces of erythrocytes and other hematopoietic cells types,[16-18] we propose that these antibodies can contribute to the destruction of red blood cells in patients with CVID with hemolytic anemia and perhaps platelets in those with thrombocytopenia, thereby potentially mediating AICs.

We thank the patients. We also thank Drs L. Devine, F. Tuluc, and C. Wang for cell sorting.

REFERENCES

1. Victora GD, Nussenzweig MC. Germinal centers. Annu Rev Immunol 2012;30:429-57.
2. Zhang Y, Meyer-Hermann M, George LA, Figge MT, Khan M, Goodall M, et al. Germinal center B cells govern their own fate via antibody feedback. J Exp Med 2013;210:457-64.
3. Cantaert T, Schickel J-N, Bannock JM, Ng Y-S, Massad C, Delmotte FR, et al. Decreased somatic hypermutation induces an impaired peripheral B cell tolerance checkpoint. J Clin Invest 2016;126:4289.
4. Zaheen A, Boulianne B, Parsa J-Y, Ramachandran S, Gommerman JL, Martin A. AID constrains germinal center size by rendering B cells susceptible to apoptosis. Blood 2009;114:547-54.
5. Bonilla FA, Barlan I, Chapel H, Costa-Carvalho BT, Cunningham-Rundles C, de la Morena MT, et al. International Consensus Document (ICON): common variable immunodeficiency disorders. J Allergy Clin Immunol Pract 2016;4:38-59.
6. Warnatz K, Denz A, Drager R, Braun M, Groth C, Wolff-Vorbeck G, et al. Severe deficiency of switched memory B cells (CD27+IgM-IgD-) in subgroups of patients with common variable immunodeficiency: a new approach to classify a heterogeneous disease. Blood 2002;99:1544-51.
7. Romberg N, Chamberlain N, Saadoun D, Gentile M, Kinnunen T, Ng YS, et al. CVID-associated TACI mutations affect autoreactive B cell selection and activation. J Clin Invest 2013;123:4283-93.
8. Schickel J-N, Glauzy S, Ng Y-S, Chamberlain N, Massad C, Isnardi I, et al. Self-reactive VH4-34-expressing IgG B cells recognize commensal bacteria. J Exp Med 2017;214:1991-2003.
9. Wardemann H, Yurasov S, Schaefer A, Young JW, Meffre E, Nussenzweig MC. Predominant autoantibody production by early human B cell precursors. Science 2003;301:1374-7.
10. Isnardi I, Ng Y-S, Menard L, Meyers G, Saadoun D, Srdanovic I, et al. Complement receptor 2/CD21- human naive B cells contain mostly autoreactive unresponsive clones. Blood 2010;115:5026-36.
11. Rakhmanov M, Keller B, Gutenberger S, Foerster C, Hoenig M, Driessen G, et al. Circulating CD21low B cells in common variable immunodeficiency resemble tissue homing, innate-like B cells. Proc Natl Acad Sci U S A 2009;106:13451-6.
12. Johansen FE, Pekna M, Norderhaug IN, Haneberg B, Hietala MA, Krajci P. Absence of epithelial immunoglobulin A transport, with increased mucosal leakiness, in polymeric immunoglobulin receptor/secretory component-deficient mice. J Exp Med 1999;190:915-22.
13. Almejún MB, Campos BC, Patiño V, Galicchio M, Zelazko M, Oleastro M, et al. Noninfectious complications in patients with pediatric-onset common variable immunodeficiency correlated with defects in somatic hypermutation but not in class-switch recombination. J Allergy Clin Immunol 2017;139:913-22.
14. Levy Y, Gupta N, Le Deist F, Garcia C, Fischer A, Weill J-C, et al. Defect in IgV gene somatic hypermutation in common variable immuno-deficiency syndrome. Proc Natl Acad Sci U S A 1998;95:13135-40.
15. Roskin KM, Simchoni N, Liu Y, Lee J-Y, Seo K, Hoh RA, et al. IgH sequences in common variable immune deficiency reveal altered B cell development and selection. Sci Transl Med 2015;7:302ra135.
16. Potter KN, Hobby P, Klijn S, Stevenson FK, Sutton BJ. Evidence for involvement of a hydrophobic patch in framework region 1 of human V4-34-encoded Igs in recognition of the red blood cell I antigen. J Immunol 2002;169:3777-82.
17. Reed JH, Jackson J, Christ D, Goodnow CC. Clonal redemption of autoantibodies by somatic hypermutation away from self-reactivity during human immunization. J Exp Med 2016;213:1255-65.

18. Sabouri Z, Schofield P, Horikawa K, Spierings E, Kipling D, Randall KL, et al. Redemption of autoantibodies on anergic B cells by variable-region glycosylation and mutation away from self-reactivity. Proc Natl Acad Sci U S A 2014;111:E2567-75.
19. Morita R, Schmitt N, Bentebibel S-E, Ranganathan R, Bourdery L, Zurawski G, et al. Human blood CXCR5(+)CD4(+) T cells are counterparts of T follicular cells and contain specific subsets that differentially support antibody secretion. Immunity 2011;34:108-21.
20. Unger S, Seidl M, Schmitt-Graeff A, Böhm J, Schrenk K, Wehr C, et al. Ill-defined germinal centers and severely reduced plasma cells are histological hallmarks of lymphadenopathy in patients with common variable immunodeficiency. J Clin Immunol 2014;34:615-26.
21. Lougaris V, Faletra F, Lanzi G, Vozzi D, Marcuzzi A, Valencic E, et al. Altered germinal center reaction and abnormal B cell peripheral maturation in PI3KR1-mutated patients presenting with HIGM-like phenotype. Clin Immunol 2015;159:33-6.
22. Yu JE, Knight AK, Radigan L, Marron TU, Zhang L, Sanchez-Ramón S. Toll-like receptor 7 and 9 defects in common variable immunodeficiency. J Allergy Clin Immunol 2009;124:349-56.
23. Nimmerjahn F, Ravetch JV. Fcgamma receptors as regulators of immune responses. Nat Rev Immunol 2008;8:34-47.
24. Perreau M, Vigano S, Bellanger F, Pellaton C, Buss G, Comte D, et al. Exhaustion of bacteria-specific CD4 T cells and microbial translocation in common variable immunodeficiency disorders. J Exp Med 2014;211:2033-45.